JCTC Journal of Chemical Theory and Computation

Comparison of Semiempirical ZILSH and DFT Calculations of Exchange Constants in the Single Molecule Magnet $[Fe_8O_2(OH)_{12}(tacn)_6]^{8+}$

Ted A. O'Brien* and Brian J. O'Callaghan

Department of Chemistry and Chemical Biology, Indiana University—Purdue University Indianapolis, 402 North Blackford Street, Indianapolis, Indiana 46202

Received March 11, 2007

Abstract: The exchange constants describing magnetic interactions between high spin Fe^{3+} ions in the complex $[Fe_8O_2(OH)_{12}(tacn)_6]^{8+}$ have been estimated with the semiempirical ZILSH method, and the results compared to those of DFT calculations and experimental magnetic studies. The ZILSH method provides more accurate estimates of the exchange constants than the DFT calculations, particularly for the "body−body" interaction within the central Fe_4 "butterfly" unit of the complex. This interaction is found to be antiferromagnetic, which contrasts with the DFT description but is in agreement with experimental studies on smaller Fe_4 butterfly complexes and known empirical correlations between exchange constants and structural parameters. The ground-state wavefunction obtained by diagonalizing the Heisenberg spin Hamiltonian matrix has a spin of ten, in agreement with previous experimental and theoretical studies. Spin alignments in the ground state demonstrate how spin frustration can lead to nonzero spin in complexes with exclusively antiferromagnetic exchange interactions.

1. Introduction

Polynuclear complexes containing transition-metal ions with unpaired spins are a subject of great interest in both nanoscale electronics and biological reaction chemistry. Coupling of the local spins of the magnetic centers can lead to high total spin ground states and the possibility of single molecule magnetism,[1−7] which could be used in nanoscale digital memory storage applications.[8] Changes in the total spin of metal clusters comprising enzyme active sites have also been implicated in important biological reactions, such as the conversion of water to free dioxygen by the water oxidizing center of the photosynthetic reaction center.[9−12] There has thus been strong motivation for the study of magnetic polynuclear transition-metal complexes, including synthesis and characterization of a growing number of single molecule magnets (SMMs) and smaller analogs of enzyme active sites.

Focusing on the SMMs, these complexes display slow reversal of magnetization at low temperature due to negative zero-field splitting of the components of a high spin ground state.[6] The size of the energy barrier for spin reversal is thus related to both the zero-field splitting parameter of the complex and the total spin of the ground state. The spin states are typically described in terms of the Heisenberg spin Hamiltonian (HSH)

$$\hat{H} = -\sum_{A<B} J_{AB}\hat{S}_A\cdot\hat{S}_B \qquad (1)$$

in which the local spin moments of the transition-metal ions (described by the local spin operators $\hat{S}_A^2$ and $\hat{S}_B^2$) couple to form states of composite total spin. The parameters $\{J_{AB}\}$ in eq 1, the exchange constants, describe the magnitude and preferred direction of magnetic coupling between paramagnetic centers labeled "A" and "B".

From an experimental perspective, estimates of the exchange constants of a complex are obtained by fitting the magnetic susceptibility measured for the complex over a range of temperatures, assuming Boltzmann-weighted populations of the spin states specified by the HSH. While certainly useful in understanding the magnetic interactions in a complex that dictate the ground-state spin and other

* Corresponding author e-mail: teobrien@indiana.edu.

10.1021/ct7000599 CCC: $37.00
Published on Web 05/10/2007

properties, this approach suffers from the problem that the great number of fitting parameters for larger complexes leads to nonunique sets of fitting parameters. There is thus need for independent methods for estimating exchange constants for magnetic polynuclear transition-metal complexes. Quantum chemistry immediately suggests itself for this purpose, since it can in principle provide information on the energetics of spin interactions from first principles.

Despite the great theoretical and computational difficulties presented by complexes containing multiple open-shell transition-metal ions, theoretical methods have increasingly played a role in the study of magnetic interactions within such complexes. It might safely be said, however, that these methods are not yet of great utility in a practical sense. Many applications of density functional theory (DFT) methods to particularly the smaller SMMs have started to appear, but these calculations are still limited in the size of complex that can be treated. A realistic practical limit is on the order of ten transition-metal ions without resorting to dividing larger complexes into smaller model fragments. Given that many larger complexes have been reported (e.g., complexes with 22 iron ions[13] and 84 manganese ions[14]), there is still a need for more efficient semiempirical methods that can accurately estimate the size and direction of magnetic couplings in large complexes.

O'Brien and Davidson recently introduced the semiempirical ZILSH formalism for treating magnetic interactions in polynuclear transition-metal complexes.[15] The formalism combines the INDO/S method of Zerner[16−23] popularized in the ZINDO program package[24] with Davidson's local spin operator[25,26] to obtain estimates of the exchange constant J_{AB} appearing in the Heisenberg spin model. ZILSH has been successfully applied to 20 iron and manganese complexes with nuclearities ranging from 2 to 12[15,27−31] but has not been systematically tested by direct comparison to experimental results for a large number of complexes. Furthermore, few comparisons with ostensibly more accurate DFT calculations are available. Larger complexes are of particular interest in this regard, as the semiempirical ZILSH method has the potential to treat complexes of much greater size than more expensive DFT calculations.

Ruiz et al. recently reported results of DFT calculations on the SMM known as Fe_8, $[Fe_8O_2(OH)_{12}(tacn)_6]^{8+}$.[32] This complex was one of the first SMMs to be characterized.[33] It has been studied in great detail both experimentally[33−36] and theoretically,[32,37] making it a good candidate for a comparative study of quantum methods. Here we report results of ZILSH calculations of the exchange constants, state energies, and spin distribution in the ground state of Fe_8. Comparisons are made with experiment and with results of the recent DFT calculations of Ruiz et al.[32]

2. Summary of Experimental Studies of Fe_8

The structure of Fe_8[33] is shown in Figure 1 (panel a) along with a schematic diagram of the exchange pathways with significant magnetic interactions (panel b). The complex is asymmetric but exhibits virtual D_2 symmetry.[34] The exchange constants can thus be approximately grouped into J_{bb}, J_A, J_B, and J_C as shown in Figure 1. All previous treatments have assumed this approximation. The bridging ligands mediating these various pathways are listed in Table 2. The central tetranuclear unit consisting of ions Fe_1-Fe_4 closely resembles the core of the well-known Fe_4 butterfly complexes.[38−42] The "body−body" interaction J_{bb} (analogous to $J_{12} = J_{bb}$ in Figure 1) in these complexes is on the order of -20 cm^{-1}, while the "wingtip-body" interactions (analogous to J_C in Figure 1) are on the order of -100 cm^{-1}.

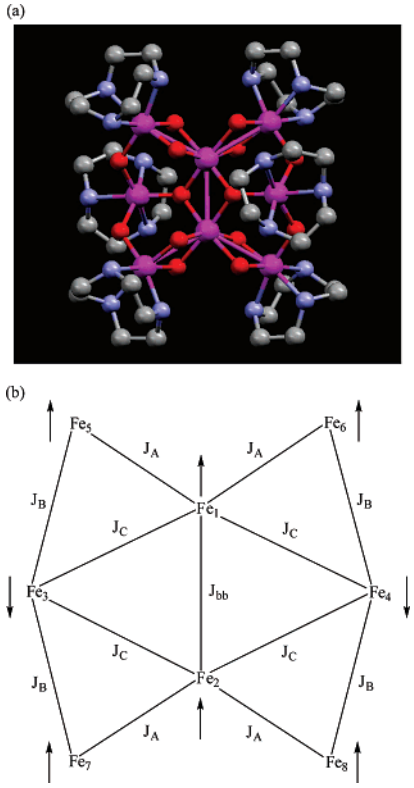

Figure 1. Structure of $[Fe_8O_2(OH)_{12}(tacn)_6]^{8+}$: (a) structural diagram (hydrogen atoms omitted for clarity). The structure was obtained from ref 33. (b) Schematic representation with labeling scheme for iron ions and exchange constants.

The magnetic properties of Fe_8 have been extensively studied with both dc and ac variable temperature magnetic susceptibility ($\chi_M T$ vs T) measurements,[34] magnetization vs magnetic field measurements at different temperatures,[34] and high-frequency electron paramagnetic resonance (EPR) measurements on both powder[34,35] and single crystal[35] samples. In early work, Delfs et al.[34] suggested a ground-state spin of $S = 10$ based on the magnetic susceptibility and magnetization curves. They interpreted the temperature dependence of the $\chi_M T$ curve at low temperature and splitting of the EPR signal at 4.2 K to indicate the presence of an excited state with a spin of $S = 9$ at very low energy. Calculations of the magnetic susceptibility were performed by diagonalizing the HSH matrix for two choices of exchange constants J_{bb}, J_A, J_B, and J_C (Figure 1). Values of $J_{bb} = -102$ cm^{-1}, $J_A = -15$ cm^{-1}, $J_B = -35$ cm^{-1}, and $J_C = -120$ cm^{-1} were found to reproduce the experimental data while predicting the presence of the excited state with a spin of $S = 9$ within 0.5 cm^{-1} of the ground state.

Barra et al. later reconsidered the interpretation described above on the basis of single-crystal high-frequency EPR

measurements.[35] They demonstrated that the low-temperature magnetic behavior of the complex is due to unusually large magnetic anisotropy in the ground state rather than the presence of a low-lying excited state. Similar behavior has also been reported for a structural analog of Fe_8.[36] Given this conclusion, exchange parameters that also reproduce the experimental $\chi_M T$ vs T curve but do not place the first excited state within a few cm^{-1} of the ground state were suggested. These values, $J_{bb} = -25\ cm^{-1}$, $J_A = -18\ cm^{-1}$, $J_B = -41\ cm^{-1}$, and $J_C = -140\ cm^{-1}$, represent the best reflection of the experimental data and are taken as "experimental" values in the following discussion. With these exchange constants, the first excited state with a spin of $S = 9$ has an energy of $24.5\ cm^{-1}$.

The ground-state wavefunction obtained by diagonalization of the HSH with the experimental values of the exchange constants gives local z-components of spin of close to $+5/2$ for ions Fe_1, Fe_2, and Fe_5-Fe_8 (see Figure 1 for labeling scheme) and $-5/2$ for Fe_3 and Fe_4.[37] These spin alignments are depicted in panel b of Figure 1. This arrangement of local spin components indicates that the J_{bb} and J_A pathways of Fe_8 are spin frustrated, as might be expected given the much larger antiferromagnetic couplings in the J_B and J_C pathways. Both the DFT calculations of Ruiz et al.[32] and the ZILSH calculations reported here agree with this picture of the spin alignments in Fe_8.

3. Theory and Methods

3.1. ZILSH Calculations. The ZILSH calculations on Fe_8 used the procedure described in ref 15. In summary, the procedure uses unrestricted Hartree Fock (UHF) molecular orbital (MO) calculations with the intermediate neglect of differential overlap Hamiltonian parametrized for optical spectroscopy (INDO/S) of Zerner.[16−23] These calculations provide single determinant wavefunctions for various spin components defined by particular alignments of the spins of the metal ions in the complex. A semiempirical application[15] of Davidson's local spin operator[25,26] is used to obtain spin couplings $\langle \hat{S}_A \cdot \hat{S}_B \rangle^{UHF}$ from the unrestricted wavefunctions. The exchange constants are then obtained assuming an effective Hamiltonian operator of the Heisenberg spin form

$$\hat{H}_{eff} = \hat{H}_0 - \sum_{A<B} J_{AB} \langle \hat{S}_A \cdot \hat{S}_B \rangle^{UHF} \quad (2)$$

where $\hat{H}_0$ contains all spin-independent terms such as electron−nuclear attraction. The expectation value of $\hat{H}_{eff}$ for the ith spin component is then

$$E^{UHF,i} = E_0 - \sum_{A<B} J_{AB} \langle \hat{S}_A \cdot \hat{S}_B \rangle^{UHF,i} \quad (3)$$

where E_0 contains all spin-independent contributions to the energy. Given energies and spin couplings for the appropriate number of spin components ($^1/_2 N_m(N_m - 1) + 1$, where N_m is the number of metal ions in the complex), the parameters E_0 and $\{J_{AB}\}$ are solved for simultaneously. Performing calculations on spin components with all unpaired spins parallel ("high spin") and with unpaired spins reversed on all unique combinations of two metal ions provides the correct number of equations for simultaneous solution for all parameters. This procedure is similar to those developed by Noodleman[43−46] and Yamaguchi,[47−49] except it calculates expectation values $\langle \hat{S}_A \cdot \hat{S}_B \rangle^{UHF}$ from the wavefunctions rather than assuming formal values.

The DFT calculations of Ruiz et al.[32] used either the hybrid B3LYP functional[50,51] or the PBE functional,[52] with the TZVP basis set of Ahlrichs[53] for the iron ions and the DZVP basis of Ahlrichs[54] for lighter atoms. A different procedure than that described above was used to obtain estimates of the exchange constants:[32] Calculations were performed for five spin components, and differences in the component energies were used to solve simultaneously for J_{bb}, J_A, J_B, and J_C (see Figure 1, panel b). This displays an important difference between the methods—the ZILSH calculations consider 29 spin components rather than five and solve for exchange constants for all unique pairwise magnetic interactions in the complex. No assumptions are made based on symmetry (e.g., setting J_{13}, J_{14}, J_{23}, and J_{24} equal to J_C; see Figure 1, panel b), and none of the interactions are arbitrarily assumed to be zero regardless of whether the two metals involved are directly bridged by ligands or not. The latter allows evaluation of second-neighbor interactions, for example, which are generally assumed to be zero. Nonzero values for second-neighbor couplings have been suggested on the basis of both experimental and theoretical evidence; see, e.g., refs 55 and 41, respectively.

3.2. Spin Eigenstates − Diagonalization of the Heisenberg Spin Hamiltonian. The spin eigenstates of the complex are obtained for a given set of exchange constants by substituting them into the HSH (eq 1) and diagonalizing the operator in the basis of spin components $\phi_i = |M_1 M_2 \cdots M_N\rangle_i$, where M_A is the local z-component of spin of the metal center labeled "A". The resulting spin state wavefunctions $|\psi_S\rangle^I$ are linear combinations of these components

$$|\psi_S\rangle^I = \sum_i C_i \phi_i = \sum_i |M_1 M_2 \cdots M_N\rangle_i \quad (4)$$

where the expansion runs over components for which the local z-components of spin add to the total spin S of the state. For smaller complexes the entire Hamiltonian matrix can readily be diagonalized to obtain energies and wavefunctions for all spin states, but this procedure becomes increasingly expensive for larger complexes. In this work we use an implementation of the Davidson algorithm[56] that efficiently provides the energy and wavefunction for the lowest energy state of each spin.

Several useful quantities can be calculated from the wavefunction of the ground (or any other) state, including the local z-component of spin of each metal, $\langle \hat{S}_{zA} \rangle$, and spin couplings $\langle \hat{S}_A \cdot \hat{S}_B \rangle$ between metal spins

$$\langle \hat{S}_{zA} \rangle = \langle \psi_S | \hat{S}_{zA} | \psi_S \rangle = \sum_i C_i^2 (M_A)_i \quad (5)$$

$$\langle \hat{S}_A \cdot \hat{S}_B \rangle = \langle \psi_S | \hat{S}_A \cdot \hat{S}_B | \psi_S \rangle = \sum_{i,j} C_i C_j \langle \phi_i | {}^1/_2 \hat{S}_A^+ \cdot \hat{S}_B^- + {}^1/_2 S_A^- \cdot \hat{S}_B^+ + \hat{S}_{zA} \cdot \hat{S}_{zB} | \phi_j \rangle \quad (6)$$

where $\hat{S}_A^+$ and $\hat{S}_A^-$ are the standard raising and lowering

Table 1. Energies and Local Spin Densities Computed from ZILSH UHF Wavefunctions for 24 Various Spin Components of the Fe_8 Complex $[Fe_8O_2(OH)_{12}(tacn)_6]^{8+}$

spin reversal[a]	energy[b] ($cm^{-}1$)	Fe_1	Fe_2	Fe_3	Fe_4	Fe_5	Fe_6	Fe_7	Fe_8
high spin	4551.64	4.39	4.39	4.26	4.27	4.20	4.19	4.19	4.19
1,2	552.46	−4.33	−4.34	4.22	4.23	4.19	4.20	4.19	4.20
1,3	1812.50	−4.36	4.37	−4.22	4.25	4.18	4.20	4.18	4.19
1,4	1820.26	−4.36	4.37	4.24	−4.23	4.19	4.19	4.19	4.18
1,5	2265.69	−4.34	4.40	4.23	4.25	−4.18	4.20	4.19	4.19
1,6	2275.51	−4.34	4.40	4.24	4.24	4.19	−4.19	4.19	4.19
1,7	1934.21	−4.34	4.39	4.23	4.25	4.19	4.20	−4.18	4.19
1,8	1981.63	−4.34	4.39	4.24	4.24	4.19	4.20	4.19	−4.19
2,3	1772.47	4.37	−4.36	−4.22	4.25	4.18	4.20	4.18	4.20
2,4	1897.81	4.37	−4.36	4.24	−4.23	4.19	4.19	4.19	4.19
2,5	1995.94	4.39	−4.34	4.23	4.25	−4.18	4.20	4.19	4.20
2,6	2037.88	4.39	−4.34	4.24	4.24	4.19	−4.19	4.19	4.20
2,7	2351.62	4.39	−4.35	4.23	4.25	4.19	4.20	−4.18	4.20
2,8	2380.07	4.39	−4.35	4.24	4.24	4.19	4.20	4.19	−4.18
3,4	0.00	4.34	4.35	−4.20	−4.21	4.18	4.19	4.18	4.18
3,5	2346.02	4.36	4.37	−4.21	4.27	−4.19	4.20	4.18	4.19
3,6	1745.03	4.36	4.37	−4.20	4.26	4.18	−4.19	4.18	4.19
3,7	2345.46	4.37	4.37	−4.21	4.27	4.18	4.20	−4.19	4.19
3,8	1775.53	4.37	4.37	−4.20	4.26	4.18	4.20	4.18	−4.19
4,5	1809.51	4.36	4.37	4.25	−4.21	−4.18	4.19	4.19	4.18
4,6	2443.86	4.36	4.37	4.26	−4.22	4.19	−4.20	4.19	4.18
4,7	1834.72	4.37	4.37	4.25	−4.21	4.19	4.19	−4.18	4.18
4,8	2426.64	4.37	4.37	4.26	-4.22	4.19	4.19	4.19	−4.20
5,6	3587.36	4.38	4.39	4.25	4.26	−4.18	−4.19	4.19	4.19
5,7	3567.76	4.38	4.39	4.24	4.27	−4.18	4.20	−4.18	4.19
5,8	3614.46	4.38	4.39	4.25	4.26	−4.18	4.20	4.19	−4.19
6,7	3607.94	4.38	4.39	4.25	4.26	4.19	−4.19	−4.18	4.19
6,8	3659.42	4.38	4.39	4.26	4.25	4.19	−4.19	4.19	−4.19
7,8	3642.71	4.39	4.38	4.25	4.26	4.19	4.20	−4.18	−4.19

[a] All spins on the indicated metals reversed relative to others; see Figure 1 panel b for the numbering scheme. [b] Relative to energy of component with all unpaired spins on Fe_3 and Fe_4 reversed.

operators for the *z*-component of spin of center A, etc. The quantity $\langle \hat{S}_{zA} \rangle$ describes the spin alignments in the state being considered. The ground-state spin couplings $\langle \hat{S}_A \cdot \hat{S}_B \rangle$ are particularly useful for identifying exchange pathways that are spin frustrated. The spin coupling indicates the actual alignment of the spin components M_A and M_B in the state, while the exchange constant J_{AB} indicates the preferred alignment. Under the $-J$ convention, then, any pathway with $\langle \hat{S}_A \cdot \hat{S}_B \rangle$ and J_{AB} of different signs is frustrated. The contribution made by an exchange pathway to the total energy of the ground state is simply $\Delta E = -J_{AB} \langle \hat{S}_A \cdot \hat{S}_B \rangle$, so a frustrated pathway increases the ground-state energy. This occurs because the resulting distribution of spins throughout the complex allows compensatory, larger decreases in energy in other pathways that are not frustrated.

4. Results and Discussion

Following the ZILSH procedure given in ref 15, an initial set of molecular orbitals (MOs) was obtained with the configuration averaged Hartree Fock (CAHF) procedure of Zerner.[57] This calculation was followed by a restricted open shell Hartree Fock (ROHF) calculation using the CAHF MOs as the starting guess. The open shell MOs obtained from the ROHF calculation, which consisted largely of iron 3d atomic orbitals, were localized with the procedure of Boys.[58−60] The resulting MOs were then used as starting guesses for unrestricted Hartree Fock (UHF) calculations on components with all unpaired spins aligned, and all cases where the unpaired spins of two metals were reversed relative to the others. These UHF calculations converged readily, each executing in minutes on the IBM JS20 processors of the Libra cluster at Indiana University.

The energies and local spin densities of the metal ions found for the 29 UHF components are presented in Table 1. The local spin densities are computed within the population analysis scheme of Löwdin[61] and are equal to twice the number of unpaired electrons on each metal. Their signs indicate alignments of the local *z*-components of spin. All values obtained are close to the formal values of ±5 expected for high spin Fe^{3+} ions and are very similar to values obtained with ZILSH for other complexes of Fe^{3+} (refs 15, 30, and 31). The absolute values of the spin densities range from 4.18 to 4.40, which are comparable to those obtained in the DFT calculations of Ruiz et al., 4.10−4.17 found with natural bond order analysis and 4.18−4.25 found with Mulliken analysis.[32] The lowest energy component is that with the spins of Fe_3 and Fe_4 reversed relative to the others (see panel b of Figure 1), in agreement with the results of Ruiz et al.[32] The component with all spins aligned has the highest energy by a considerable margin, indicating that the magnetic interactions in the complex are predominantly antiferromagnetic.

Table 2. Exchange Constants Obtained for the Fe_8 Complex from ZILSH and DFT Calculations and from Experimental Magnetic Susceptibility Data and Ground-State Spin Couplings Obtained from Diagonalization of the Heisenberg Spin Hamiltonian with ZILSH Exchange Constants

parameter[a]		type of interaction	J_{PBE}[b] (cm^{-1})	J_{B3LYP}[b]	J_{ZILSH}[c]	$\langle \hat{S}_A \cdot \hat{S}_B \rangle$[d]	J_{exp}[e]
J_{bb}	J_{12}	$(O^{2-})_2$	+28.9	+5.1	−9.4	+6.25	−25
J_A	J_{15}	$(OH^-)_2$	−9.2	−10.4	−19.3	+5.58	−18
	J_{16}				−17.5	+5.56	
	J_{27}				−17.9	+5.61	
	J_{28}				−16.8	+5.58	
J_B	J_{35}	OH^-	−14.4	−34.1	−36.4	−6.00	−41
	J_{37}				−34.0	−5.99	
	J_{46}				−33.2	−5.97	
	J_{48}				−30.6	−5.89	
J_C	J_{13}	O^{2-}	−55.8	−66.5	−94.7	−7.24	−140
	J_{14}				−89.0	−7.22	
	J_{23}				−87.8	−7.17	
	J_{24}				−88.4	−7.25	

[a] See Figure 1, panel b for numbering scheme. [b] Reference 32. [c] This work. [d] Computed from the ground-state wavefunction obtained by diagonalizing the HSH with ZILSH exchange constants. [e] Reference 36.

Spin couplings $\langle \hat{S}_A \cdot \hat{S}_B \rangle^{UHF}$ computed for the 29 spin components listed in Table 1 are given as Supporting Information. All values are close to ±4.5, which are typical of values obtained with ZILSH for other complexes of Fe^{3+} (refs 15, 30, and 31). Along with the component energies of Table 1, these spin couplings allow all exchange constants in the complex to be obtained through simultaneous solution of eq 3. All nonzero exchange constants found are presented in Table 2, along with those found with DFT by Ruiz et al.[32] and those fit to the experimental magnetic susceptibility data.[35]

Considering first the ZILSH exchange constants for all pathways, some minor variations in values were found within the subgroups J_A, J_B, and J_C, reflecting the actual lack of symmetry in the complex. These variations are uniformly small, indicating that the assumption of equivalent interactions is a good approximation for this complex. Turning to a comparison of calculated values with experiment, it is apparent from Table 2 that the ZILSH exchange constants compare more favorably with the experimental values than the DFT values. Comparing results obtained with the two functionals, it appears that the hybrid B3LYP functional performs better than the PBE functional, particularly for the hydroxide-mediated interaction J_B and the oxide-mediated interaction J_{bb}.

The DFT calculations suggest that J_{bb}, the "body−body" interaction within the central Fe_4 butterfly cluster of the complex, might be weakly ferromagnetic. This is not supported by experimental results for known Fe_4 butterfly complexes, which all have small but antiferromagnetic couplings ranging between -11 cm^{-1} and -21 cm^{-1}.[38,39,62−64] It should be pointed out, however, that the quality of fits of magnetic susceptibility data for these complexes is relatively insensitive to the value of J_{bb}. In the case of the complex $[Fe_4O_2(O_2CMe)_7(bpy)_2]^+$, for example, McCusker et al.[39] could only conclude that J_{bb} is more positive than -15 cm^{-1} and likely to be antiferromagnetic. The experimental results can thus not be assumed to be definitive for these complexes regarding the sign of J_{bb}.

Further insight regarding the value and sign of the exchange constant J_{bb} in Fe_8 can be gained by looking at existing relationships between exchange constants and structural parameters such as Fe−O distances (r) and Fe−O−Fe angles (ϕ) in bridging pathways. Several such "magnetostructural correlations" have been presented in the literature. Gorun and Lippard[65] considered 36 complexes with two or three Fe^{3+} ions and both substituted and unsubstituted oxide bridging ligands and found a correlation between Fe−O distance and J

$$-J = (1.7526 \times 10^{12}\ cm^{-1}) \exp(-12.633\ Å^{-1} \cdot P) \quad (7)$$

where P is "half the shortest distance of the superexchange pathway between two metals". Weihe and Güdel[66] considered 32 oxide-bridged Fe^{3+} dimer complexes with exchange constants ranging from -160 cm^{-1} to -265 cm^{-1} and found a relationship between J and both Fe−O distance and Fe−O−Fe angle

$$-J = (1.337 \times 10^{8}\ cm^{-1})\,(3.536 + 2.488\cos(\phi) + \cos^2(\phi))\exp(-7.909\ Å^{-1} \cdot \bar{r}) \quad (8)$$

where $\bar{r}$ is the average Fe−O distance for the exchange pathway. Cañada-Vilalta et al.[31] considered a correlation between J and Fe−O distance and Fe−O−Fe angle in four hexanuclear Fe^{3+} complexes with substituted and unsubstituted oxide bridging interactions, obtaining

$$-J = (2 \times 10^{7}\ cm^{-1})\,(0.2 - \cos(\phi) + \cos^2(\phi))\exp(-7\ Å^{-1} \cdot \bar{r}) \quad (9)$$

where $\bar{r}$ and ϕ are the average Fe−O distance and Fe−O−Fe angle for the shortest bridging pathway between two metals.

Estimates of the exchange constant J_{bb} of Fe_8 obtained from eqs 7−9 are collected in Table 3 along with the various geometric parameters used. Values between -16 and -77 cm^{-1} are obtained. Among these, the value of -77 cm^{-1} obtained from eq 8 seems too large in magnitude and might be considered least reliable given that the correlation included only dimer complexes with $|J|$ greater than 160 cm^{-1}, and $\bar{r}$ and ϕ values quite different from those found for the J_{bb} pathway in Fe_8.[66] The correlation of Gorun and Lippard[65] included interactions mediated by unsubstituted oxide ligands with exchange constants ranging from -52 cm^{-1} to -264 cm^{-1} as well as interactions mediated by substituted oxide ligands with J as low as -14 cm^{-1} so is likely more applicable to J_{bb} in Fe_8. The correlation of Cañada-Vilalta et al.[31] is perhaps the most reliable, as it is based on interactions in polynuclear complexes that are structurally similar to Fe_8, with exchange constants for $Fe-O^{2-}-Fe$ interactions as low as -8 cm^{-1}. The latter two correlations predict values of -31 cm^{-1} and -16 cm^{-1} for J_{12} in Fe_8, respectively. Given that J_{bb} found to closely reproduce the experimental $\chi_M T$ curve of Fe_8 is -25 cm^{-1},[35] the ZILSH calculations estimate a value of -10 cm^{-1} (Table 2), and

Table 3. Exchange Constant J_{bb} (See Figure 1, Panel b for the Labeling Scheme) of the Fe_8 Complex Estimated with Various Magnetostructural Correlations[f]

formula	geometric parameter(s)		J_{12} (cm^{-1})	ref
$-J = (1.7526 \times 10^{12}\ cm^{-1}) \exp(-12.633\ Å^{-1} \cdot P)$	P[a] = 1.9565 Å		−30.5	67
$-J = (1.337 \times 10^{8}\ cm^{-1})\ (3.536 + 2.488 \cos(\phi) + \cos^2(\phi))\ \exp(-7.909\ Å^{-1} \cdot \bar{r})$	$\bar{r}$[b] = 1.96525 Å	ϕ[c] = 96.81°	−77.3	68
$-J = (2 \times 10^{7}\ cm^{-1})\ (0.2 - \cos(\phi) + \cos^2(\phi))\ \exp(-7\ Å^{-1} \cdot \bar{r})$	$\bar{r}$[d] = 1.9565 Å	ϕ[e] = 97.38°	−15.6	31

[a] "Half the shortest distance of the superexchange pathway between two metals." (ref 67). [b] Average Fe−O distance in the exchange pathway. [c] Average Fe−O−Fe angle in the exchange pathway. [d] Average Fe−O distance in the shortest bridging pathway. [e] Average Fe−O−Fe angle in the shortest bridging pathway. [f] Structural parameters were obtained from ref 33.

Table 4. Local *z*-Components of Spin $\langle \hat{S}_{zA} \rangle$ and Energy Difference between Ground and First Excited State Computed from the Ground-State Wavefunction Obtained by Diagonalizing the HSH with Exchange Constants Obtained from Various Methods

z-component	PBE[a]	B3LYP[a]	ZILSH[b]	(exp)[c]
$\langle \hat{S}_{z1} \rangle$[d]	3.72	4.46	4.15	4.06
$\langle \hat{S}_{z2} \rangle$	3.72	4.46	4.18	4.06
$\langle \hat{S}_{z3} \rangle$	−3.65	−4.28	−4.04	−3.98
$\langle \hat{S}_{z4} \rangle$	−3.65	−4.28	−4.04	−3.98
$\langle \hat{S}_{z5} \rangle$	4.97	4.91	4.95	4.96
$\langle \hat{S}_{z6} \rangle$	4.97	4.91	4.94	4.96
$\langle \hat{S}_{z7} \rangle$	4.97	4.91	4.94	4.96
$\langle \hat{S}_{z8} \rangle$	4.97	4.91	4.94	4.96
ΔE, $S = 10 \rightarrow S = 9$ (cm^{-1})	4.5	30.5	17.4	24.5

[a] Reference 32. [b] This work. [c] Reference 36. [d] See Figure 1, panel b for the numbering scheme.

J_{bb} in Fe_4 butterfly complexes with Fe−O−Fe structural parameters similar to those for the J_{bb} pathway of Fe_8 ranges from $-11\ cm^{-1}$ to $-21\ cm^{-1}$ (see above), it seems unlikely that J_{bb} is ferromagnetic, as estimated by the DFT calculations reported in ref 32.

The above discussion suggests that the DFT calculations, particularly those with the PBE functional, are overestimating the ferromagnetic contribution to the exchange constant J_{bb} in Fe_8. This might indicate a general tendency of DFT—a similar result was reported for the complex $[Fe_4O_2(O_2CMe)_7(bpy)_2]^+$, for which B3LYP calculations using the TZVP basis set[53] for the iron ions and the DZVP basis set[54] on lighter atoms (the same basis set used in ref 32 for Fe_8) gave $J_{bb} = +8.3\ cm^{-1}$,[41] versus $-18.8\ cm^{-1}$ from a fit of the experimental $\chi_M T$ curve measured for the complex.[39] ZILSH calculations on this complex gave $J_{bb} = -12.0\ cm^{-1}$.[15] The ZILSH method thus appears to slightly overestimate the ferromagnetic contribution to J_{bb} in Fe_8 and $[Fe_4O_2(O_2CMe)_7(bpy)_2]^+$ but not to the extent that the DFT methods do. More testing with additional complexes will be needed to confirm these conclusions about the performance of the methods.

Wavefunctions for the lowest energy state of each spin of the complex were obtained by substituting the exchange constants of Table 2 into the HSH (eq 1) and diagonalizing in the basis of spin components (eq 4). Results obtained from these calculations are presented in Table 4. The ground state has a spin of $S = 10$, in agreement with previous experimental[34,35] and theoretical[32,37] studies. The first excited state has a spin of $S = 9$, also as suggested previously,[32,34,35,37] and is 17.4 cm^{-1} above the ground state in energy. This compares favorably with both experiment (24.5 cm^{-1}; ref 35) and DFT calculations with the B3LYP functional (30.5 cm^{-1}). The PBE functional predicts a smaller energy difference (4.5 cm^{-1}).[32]

The ground-state wavefunction obtained by diagonalizing the HSH with the ZILSH exchange constants consists primarily of the component in which the spins of Fe_3 and Fe_4 are reversed relative to the others. Its form is

$$|\psi_{S=10}\rangle = 0.70\left|\frac{5}{2},\frac{5}{2},-\frac{5}{2},-\frac{5}{2},\frac{5}{2},\frac{5}{2},\frac{5}{2},\frac{5}{2}\right\rangle - 0.24\left|\frac{5}{2},\frac{3}{2},-\frac{5}{2},-\frac{3}{2},\frac{5}{2},\frac{5}{2},\frac{5}{2},\frac{5}{2}\right\rangle - 0.24\left|\frac{5}{2},\frac{3}{2},-\frac{3}{2},-\frac{5}{2},\frac{5}{2},\frac{5}{2},\frac{5}{2},\frac{5}{2}\right\rangle - 0.24\left|\frac{3}{2},\frac{5}{2},-\frac{5}{2},-\frac{3}{2},\frac{5}{2},\frac{5}{2},\frac{5}{2},\frac{5}{2}\right\rangle - 0.24\left|\frac{3}{2},\frac{5}{2},-\frac{3}{2},-\frac{5}{2},\frac{5}{2},\frac{5}{2},\frac{5}{2},\frac{5}{2}\right\rangle + \cdots \quad (10)$$

The rest of the wavefunction is comprised of a large number of components with much smaller coefficients. This wavefunction has the same leading component as that obtained by Barra et al.[35] with the experimental exchange constants but differs slightly in the relative magnitudes of the coefficients for those components making smaller contributions. The two wavefunctions predict very similar properties, however—both the local *z*-components of spin $\langle \hat{S}_{zA} \rangle$ and the energy difference between the ground state and the first excited state are very similar for the two wavefunctions (see the right two columns of Table 4). Wavefunctions obtained with the DFT exchange constants also give similar values for the local *z*-components of spin.

The wavefunctions obtained with the experimental and various theoretical exchange constants all display the same ground-state spin alignments, with the local spins of Fe_3 and Fe_4 reversed relative to the others. This leads to the total ground-state spin of $S = 10$. According to the ZILSH and the experimental exchange constants, the J_{bb} and four J_A pathways are spin frustrated, as seen from the spin couplings $\langle \hat{S}_A \cdot \hat{S}_B \rangle$ computed from the ground-state wavefunction (sixth column of Table 2): $\langle \hat{S}_A \cdot \hat{S}_B \rangle$ and J_{AB} differ in sign for these pathways, while they carry the same sign for the other pathways. This occurs because of the relatively small magnitudes of J_{bb} and J_A relative to those of J_B and J_C.

It is interesting to note that $\langle \hat{S}_1 \cdot \hat{S}_2 \rangle$, the spin coupling between metal ions in the J_{bb} pathway in the ground state, takes on a value of exactly +6.25 (Table 2). This is the formal value expected for two noninteracting particles with local spin quantum numbers of $S_A = S_B = 5/2$. This occurs because the very small J_{bb} interaction between Fe_1 and Fe_2 of $-9.4\ cm^{-1}$ is completely overwhelmed by the four much larger J_C interactions of ca. $-100\ cm^{-1}$ in the central butterfly unit. The interaction between Fe_1 and Fe_2 is thus rendered insignificant, and the two ions display the spin coupling

of two noninteracting particles with $S_A = S_B = 5/2$. The J_A pathways are also frustrated but with spin couplings that deviate from the value expected for noninteracting particles with $S_A = S_B = 5/2$. Viewed in this way, the J_{bb} pathway could be said to be completely frustrated in Fe_8, while the J_A pathways are largely (but not completely) frustrated.

In general, the Fe_8 complex is a good example of how a large ground-state spin can occur in a complex in which all magnetic interactions are antiferromagnetic. The mechanism of this is spin frustration caused by competing antiferromagnetic exchange interactions of different magnitudes. In the case of Fe_8, the topology of the complex leads to five adjacent pathways that are spin frustrated (the J_{bb} and four J_A pathways; see Figure 1), so that the six local spin components of Fe_1, Fe_2, and Fe_5-Fe_8 are aligned parallel in the ground state. The locations of the spin frustrated pathways are thus crucial to building up an appreciable spin moment in a complex with exclusively antiferromagnetic interactions—if the J_{bb} and J_C pathways were spin frustrated rather than the J_{bb} and J_A pathways, for example, the spins of Fe_1-Fe_4 would be aligned parallel to each other and antiparallel to the spins of Fe_5-Fe_8, and the spin of the ground state would be zero.

5. Conclusions

The exchange constants describing magnetic interactions between high spin Fe^{3+} ions in the single molecule magnet $[Fe_8O_2(OH)_{12}(tacn)_6]^{8+}$ have been estimated with the semiempirical ZILSH method. The resulting values were compared to those obtained from DFT calculations[32] as well as those fit to reproduce experimental magnetic data.[35] The ZILSH calculations were performed for 29 spin components of the complex, allowing exchange constants for all pairwise interactions to be solved for. This contrasts with the DFT calculations, which grouped together exchange constants that are approximately equivalent by symmetry, neglected others presumed to have zero magnitude, and considered only five spin components.[32] Spin densities obtained for the metal ions for these spin components with ZILSH and DFT were very similar. The component with all unpaired spins aligned parallel was found to be considerably higher in energy than all others with both methods, indicating that the magnetic interactions are predominantly antiferromagnetic.

A number of conclusions can be drawn by comparing the exchange constants obtained from ZILSH and DFT calculations and from fitting to reproduce the experimental magnetic data. First, the exchange constants obtained with ZILSH show that the approximation of grouping exchange constants together into J_{bb}, J_A, J_B, and J_C (see Figure 1 and Table 1) is a good approximation for this complex. Second, the exchange constants obtained with ZILSH are consistently closer to those obtained from the experimental data than those obtained from the DFT calculations. Comparing the two functionals used in ref 32, the hybrid B3LYP functional performs better than the PBE functional for this complex.

Both DFT functionals indicate that J_{bb}, the "body−body" interaction within the central Fe_4 butterfly unit of Fe_8, is weakly ferromagnetic.[32] The ZILSH calculations, by contrast, indicate that this interaction is weakly antiferromagnetic. This is supported by experimental magnetic data for known Fe_4 butterfly complexes[38,39,62−64] and established correlations between exchange constants and structural parameters within the bridging pathways.[31,65,66] There could be a general tendency of DFT methods to overestimate ferromagnetic contributions to exchange constants of small magnitude, as a similar result was reported for the butterfly complex $[Fe_4O_2(O_2CMe)_7(bpy)_2]^+$ (ref 41). Further testing of both ZILSH and DFT for other complexes is needed to further investigate this question.

Substitution of the exchange constants obtained with ZILSH into the Heisenberg spin Hamiltonian and diagonalization gives a ground state with a spin of $S = 10$ and a first excited state with spin of $S = 9$ that is 17.4 cm^{-1} above the ground state in energy. This is in close agreement with both experiment[35] and the B3LYP calculations.[32] Spin alignments in the ground state are similar for all sets of exchange constants (ZILSH, DFT,[32] and experimental[35,37] values) and are arranged as shown in panel b of Figure 1. The J_{bb} and J_A pathways are spin frustrated, leading to parallel alignment of the spins of Fe_1, Fe_2, and Fe_5-Fe_8 and hence the ground-state spin of $S = 10$.

The ability of quantum chemical methods such as ZILSH and DFT to provide detailed analysis of magnetic interactions in large complexes could eventually be useful in the rational design of single molecule magnets with desirable properties such as high blocking temperatures for spin reversal. The ZILSH method is very efficient and could in principle be applied to much larger complexes than DFT methods. We are currently performing ZILSH calculations on complexes with nuclearities as high as 22 to demonstrate this capability.

Acknowledgment. This work was supported in part by Shared University Research grants from IBM, Inc. to Indiana University.

Supporting Information Available: Spin couplings $\langle \hat{S}_A \cdot \hat{S}_B \rangle$ computed from UHF wavefunctions for spin components with all unpaired spins aligned and all cases with unpaired spins on pairs of metal ions reversed (Table S1). This material is available free of charge via the Internet at http://pubs.acs.org.

References

(1) Sessoli, R.; Tsai, H. L.; Schake, A. R.; Wang, S. Y.; Vincent, J. B.; Folting, K.; Gatteschi, D.; Christou, G.; Hendrickson, D. N. *J. Am. Chem. Soc.* **1993**, *115*, 1804−1816.

(2) Sessoli, R.; Gatteschi, D.; Caneschi, A.; Novak, M. A. *Nature* **1993**, *365*, 141−143.

(3) Sangregorio, C.; Ohm, T.; Paulsen, C.; Sessoli, R.; Gatteschi, D. *Phys. Rev. Lett.* **1997**, *78*, 4645−4648.

(4) Eppley, H. J.; Tsai, H. L.; Devries, N.; Folting, K.; Christou, G.; Hendrickson, D. N. *J. Am. Chem. Soc.* **1995**, *117*, 301−317.

(5) Caneschi, A.; Gatteschi, D.; Sessoli, R.; Barra, A. L.; Brunel, L. C.; Guillot, M. *J. Am. Chem. Soc.* **1991**, *113*, 5873−5874.

(6) Beltran, L. M. C.; Long, J. R. *Acc. Chem. Res.* **2005**, *38*, 325−334.

(7) Barra, A. L.; Debrunner, P.; Gatteschi, D.; Schulz, C. E.; Sessoli, R. *Europhys. Lett.* **1996**, *35*, 133−138.

(8) Leuenberger, M. N.; Loss, D. *Nature* **2001**, *410*, 789−793.

(9) Yagi, M.; Kaneko, M. *Chem. Rev.* **2001**, *101*, 21−35.

(10) Yachandra, V. K.; Sauer, K.; Klein, M. P. *Chem. Rev.* **1996**, *96*, 2927−2950.

(11) Ruttinger, W.; Dismukes, C. G. *Chem. Rev.* **1997**, *97*, 1−24.

(12) Manchanda, R.; Brudvig, G. W.; Crabtree, R. H. *Coord. Chem. Rev.* **1995**, *144*, 1−38.

(13) Foguet-Albiol, D.; Abboud, K. A.; Christou, G. *Chem. Commun.* **2005**, 4282−4284.

(14) Tasiopoulos, A. J.; Vinslava, A.; Wernsdorfer, W.; Abboud, K. A.; Christou, G. *Angew. Chem., Int. Ed. Engl.* **2004**, *43*, 2117−2121.

(15) O'Brien, T. A.; Davidson, E. R. *Int. J. Quantum Chem.* **2003**, *92*, 294−325.

(16) Zerner, M. C.; Loew, G. H.; Kirchner, R. F.; Muellerwesterhoff, U. T. *J. Am. Chem. Soc.* **1980**, *102*, 589−599.

(17) Ridley, J. E.; Zerner, M. C. *Theor. Chim. Acta* **1973**, *32*, 111−134.

(18) Kotzian, M.; Rosch, N.; Zerner, M. C. *Theor. Chim. Acta* **1992**, *81*, 201−222.

(19) Culberson, J. C.; Knappe, P.; Rosch, N.; Zerner, M. C. *Theor. Chim. Acta* **1987**, *71*, 21−39.

(20) Cory, M. G.; Kostlmeier, S.; Kotzian, M.; Rosch, N.; Zerner, M. C. *J. Chem. Phys.* **1994**, *100*, 1353−1365.

(21) Bacon, A. D.; Zerner, M. C. *Theor. Chim. Acta* **1979**, *53*, 21−54.

(22) Anderson, W. P.; Cundari, T. R.; Zerner, M. C. *Int. J. Quantum Chem.* **1991**, *39*, 31−45.

(23) Anderson, W. P.; Cundari, T. R.; Drago, R. S.; Zerner, M. C. *Inorg. Chem.* **1990**, *29*, 1−3.

(24) Zerner, M. C.; Ridley, J. E.; Bacon, A. D.; Edwards, W. D.; Head, J. D.; McKelvey, J.; Culberson, J. C.; Knappe, P.; Cory, M. G.; Weiner, B.; Baker, J. D.; Parkinson, W. A.; Kannis, D.; Yu, J.; Rosch, N.; Kotzian, M.; Tamm, T.; Karelson, M. M.; Zheng, X.; Pearl, G. M.; Broo, A.; Albert, K.; O'Brien, T. A.; Cullen, J. M.; Cramer, C. J.; Truhlar, D. G.; Li, J.; Hawkins, G. D.; Liotard, D. A. *ZINDO-A Semi-Empirical Program Package*; University of Florida: Gainesville, FL, 2000.

(25) Davidson, E. R.; Clark, A. E. *Mol. Phys.* **2002**, *100*, 373−383.

(26) Clark, A. E.; Davidson, E. R. *J. Chem. Phys.* **2001**, *115*, 7382−7392.

(27) Tasiopoulos, A. J.; O'Brien, T. A.; Abboud, K. A.; Christou, G. *Angew. Chem., Int. Ed. Engl.* **2004**, *43*, 345−349.

(28) Foguet-Albiol, D.; O'Brien, T. A.; Wernsdorfer, W.; Moulton, B.; Zaworotko, M. J.; Abboud, K. A.; Christou, G. *Angew. Chem., Int. Ed. Engl.* **2005**, *43*, 897−901.

(29) Canada-Vilalta, C.; Streib, W. E.; Huffman, J. C.; O'Brien, T. A.; Davidson, E. R.; Christou, G. *Inorg. Chem.* **2004**, *43*, 101−115.

(30) Canada-Vilalta, C.; O'Brien, T. A.; Pink, M.; Davidson, E. R.; Christou, G. *Inorg. Chem.* **2003**, *42*, 7819−7829.

(31) Canada-Vilalta, C.; O'Brien, T. A.; Brechin, E. K.; Pink, M.; Davidson, E. R.; Christou, G. *Inorg. Chem.* **2004**, *43*, 5505−5521.

(32) Ruiz, E.; Cano, J.; Alvarez, S. *Chem. Eur. J.* **2005**, *11*, 4767−4771.

(33) Wieghardt, K.; Pohl, K.; Jibril, I.; Huttner, G. *Angew. Chem., Int. Ed. Engl.* **1984**, *23*, 77−78.

(34) Delfs, C.; Gatteschi, D.; Pardi, L.; Sessoli, R.; Wieghardt, K.; Hanke, D. *Inorg. Chem.* **1993**, *32*, 3099−3103.

(35) Barra, A. L.; Gatteschi, D.; Sessoli, R. *Chem. Eur. J.* **2000**, *6*, 1608−1614.

(36) Barra, A. L.; Bencini, F.; Caneschi, A.; Gatteschi, D.; Paulsen, C.; Sangregorio, C.; Sessoli, R.; Sorace, L. *ChemPhysChem* **2001**, *2*, 523−531.

(37) Raghu, C.; Rudra, I.; Sen, D.; Ramasesha, S. *Phys. Rev. B* **2001**, *64*, 064419.

(38) Wemple, M. W.; Coggin, D. K.; Vincent, J. B.; McCusker, J. K.; Streib, W. E.; Huffman, J. C.; Hendrickson, D. N.; Christou, G. *J. Chem. Soc., Dalton Trans.* **1998**, 719−725.

(39) McCusker, J. K.; Vincent, J. B.; Schmitt, E. A.; Mino, M. L.; Shin, K.; Coggin, D. K.; Hagen, P. M.; Huffman, J. C.; Christou, G.; Hendrickson, D. N. *J. Am. Chem. Soc.* **1991**, *113*, 3012−3021.

(40) Gorun, S. M.; Lippard, S. J. *Inorg. Chem.* **1988**, *27*, 149−156.

(41) Cauchy, T.; Ruiz, E.; Alvarez, S. *J. Am. Chem. Soc.* **2006**, *128*, 15722−15727.

(42) Armstrong, W. H.; Roth, M. E.; Lippard, S. J. *J. Am. Chem. Soc.* **1987**, *109*, 6318−6326.

(43) Zhao, X. G.; Richardson, W. H.; Chen, J. L.; Li, J.; Noodleman, L.; Tsai, H. L.; Hendrickson, D. N. *Inorg. Chem.* **1997**, *36*, 1198−1217.

(44) Noodleman, L.; Norman, J. G. *J. Chem. Phys.* **1979**, *70*, 4903−4906.

(45) Noodleman, L.; Davidson, E. R. *Chem. Phys.* **1986**, *109*, 131−143.

(46) Noodleman, L. *J. Chem. Phys.* **1981**, *74*, 5737−5743.

(47) Yamaguchi, K.; Fukui, H.; Fueno, T. *Chem. Lett.* **1986**, 625−628.

(48) Yamaguchi, K. *Chem. Phys. Lett.* **1975**, *33*, 330−335.

(49) Soda, T.; Kitagawa, Y.; Onishi, T.; Takano, Y.; Nagao, H.; Yoshioka, Y.; Yamaguchi, K. *Chem. Phys. Lett.* **2000**, *319*, 223−230.

(50) Lee, C.; Yang, W.; Parr, R. G. *Phys. Rev. B* **1988**, *37*, 785−789.

(51) Becke, A. D. *J. Chem. Phys.* **1993**, *98*, 5648−5652.

(52) Perdew, J.; Burke, K.; Ernzerhof, M. *Phys. Rev. Lett.* **1996**, *77*, 3865−3868.

(53) Schaefer, A.; Huber, C.; Ahlrichs, R. *J. Chem. Phys.* **1994**, *100*, 5829−5835.

(54) Schaefer, A.; Horn, H.; Ahlrichs, R. *J. Chem. Phys.* **1992**, *97*, 2571−2577.

(55) Barra, A. L.; Caneschi, A.; Cornia, A.; Fabrizi de Biani, F.; Gatteschi, D.; Sangregorio, C.; Sessoli, R.; Sorace, L. *J. Am. Chem. Soc.* **1999**, *121*, 5302−5310.

(56) Davidson, E. R. *J. Comput. Phys.* **1975**, *17*, 87−94.

(57) Zerner, M. C. *Int. J. Quantum Chem.* **1989**, *35*, 567−575.

(58) Boys, S. F. *Rev. Mod. Phys.* **1960**, *32*, 305−307.

(59) Boys, S. F. *Rev. Mod. Phys.* **1960**, *32*, 300−302.

(60) Boys, S. F. *Rev. Mod. Phys.* **1960**, *32*, 296−299.

(61) Löwdin, P.-O. *J. Chem. Phys.* **1950**, *18*, 365−375.

(62) Yan, B.; Chen, Z. D. *Inorg. Chem. Commun.* **2001**, *4*, 138−141.

(63) Boudalis, A. K.; Tangoulis, V.; Raptopoulous, C. P.; Terzis, A.; Tuchagues, J. P.; Perlepes, S. P. *Inorg. Chim. Acta* **2004**, *357*, 1345−1354.

(64) Boudalis, A. K.; Lalioti, N.; Spyroulias, G. A.; Raptopoulous, C. P.; Terzis, A.; Bousseksou, A.; Tangoulis, V.; Tucagues, J. P.; Perlepes, S. P. *Inorg. Chem.* **2002**, *41*, 6474−6487.

(65) Gorun, S. M.; Lippard, S. J. *Inorg. Chem.* **1991**, *30*, 1625−1630.

(66) Weihe, H.; Güdel, H. U. *J. Am. Chem. Soc.* **1997**, *119*, 6539−6543.

CT7000599